

Surgical Timing Prediction of Patient-Specific Congenital Tracheal Stenosis with Bridging Bronchus by Using Computational Aerodynamics

Juanya Shen¹, Limin Zhu¹, Zhirong Tong¹, Jinfen Liu¹, Mitsuo Umezū²,
Zhuomin Xu^{1(✉)}, and Jinlong Liu^{1,3(✉)}

¹ Department of Cardiothoracic Surgery, Shanghai Children's Medical Center, Shanghai Jiao Tong University School of Medicine, 1678 Dongfang Road, Shanghai 200127, China
zmxymb@163.com, jinlong_liu_man@163.com

² Center for Advanced Biomedical Sciences, TWIns, Waseda University,
03C-301, ASMeW Lab 2-2 Wakamatsucho, Shinjuku, Tokyo 162-8480, Japan

³ Institute of Pediatric Translational Medicine, Shanghai Children's Medical Center, Shanghai Jiao Tong University School of Medicine, 1678 Dongfang Road, Shanghai 200127, China

Abstract. Congenital tracheal stenosis (CTS) has a high clinical mortality in neonates and infants. Although the procedure of slide tracheoplasty (STP) applied over the years, it is still a challenge for clinicians to predict the surgical timing of the CTS correction. In the present study, we studied on three-dimensional (3D) aerodynamic analysis of an original tracheal model from a specific patient with CTS and bridging bronchus (BB) and four new reconstructed models. We constructed a 3D patient-specific tracheal model based on CT images and applied computer-aided design (CAD) to reconstruct four models to imitate the stenosis development of CTS. Average pressure drop (APD), wall shear stress (WSS) and velocity streamlines were calculated to analyze local aerodynamic characteristics for the evaluation of airflow at the inspiration phase and expiration phase, respectively. We found APD, WSS and AEL decreased during the respiration with the decrease of stenosis. Three abnormal gradients in APD were observed between the main stenosis of trachea arrived at 80% and 60%. This implied the surgical correction may be required when the main stenosis reached 60%. The combination of CAD and aerodynamic analysis is a potential noninvasive tool for surgical timing prediction in the management of patient-specific correction of CTS.

Keywords: Congenital tracheal stenosis · Computational fluid dynamics · Aerodynamics · Computer-aided design · Airflow

1 Introduction

Congenital tracheal stenosis (CTS) that would endanger respiratory function of children is a critical and life-threatening disease. In view of the multiformity of clinical

J. Shen and L. Zhu—Co-first author

manifestation, complexity of tracheal abnormalities and its rarity, a reasonable and efficient treatment of CTS is a great challenge to surgeons [1–3]. CTS with bridging bronchus (BB) is the most challenging type of CTS, which sometimes causes high morbidity and mortality. At present, surgeons usually determine the surgical timing of CTS with BB depend on their own experience in clinical medicine and equipment inspection, which is hard to avoid the occurrence of misdiagnosis [3]. Recent years, the technology of image processing and numerical analysis [4] has played an increasingly important role in the areas of medical diagnoses and therapies and largely improves the possibility of pre-operative evaluation of aerodynamic outcomes of CTS [5–7]. Therefore, it is necessary to combine multiple disciplines to make a timely and effective approach for the patient with CTS.

In the present study, our research focused on the analysis of patient-specific tracheal aerodynamics. Three-dimensional 3D model with CTS before surgery was reconstructed. We defined it as the original model with 60% stenosis. According to the model, we imitated four stages of stenosis development (models with non-stenosis, 20% stenosis, 40% stenosis and 80% stenosis, respectively). Computational fluid dynamics (CFD) as a noteworthy method was used to simulate the tracheal aerodynamics. Average pressure drop (APD), wall shear stress (WSS) and velocity streamlines at the inspiration phase and expiration phase were calculated to evaluate the local aerodynamic characteristics for the analysis of the impairment of airflow in trachea. The major objection of the present study is to introduce our methods for the surgical timing prediction of CTS by computational aerodynamics.

2 Materials and Methods

2.1 Patient Information Acquisition

In the present study, a male little child was diagnosed with PAS which was associated with CTS, complete tracheal rings and BB, when he was 15-month-old. With the informed agreement from the parents and the local institutional review board and regional research ethics committee of Shanghai Children's Medical Center (SCMC) Affiliated Shanghai Jiao Tong University School of Medicine our research was agreed to be carried out.

As to image acquisition equipment, 16-slice multi-detector row enhanced CT scanner (Bright Speed Elite, GE Medical System, General Electric, America) was utilized to acquire the patient-specific CT images. Scanning parameters included the thickness of each slice 0.625 mm and CT image resolution 512×512 pixels. CT images were preserved in DICOM format.

2.2 Generation of Geometric Models

Medical imaging software, Materialise[®]-Mimics 18.0, was used to compile and reconstruct the patient-specific tracheal model. By this step, a patient-specific model was visualized and transformed into 3D geometry from 2D images. After with an exact measurement in the original CT image, a 3D tracheal model of the 2-generation airway

(bronchial tree) with high accuracy was reconstructed. The 3D tracheal model after surface smoothing is shown in Fig. 1, which can be observed clearly with three stenosis: Main Stenosis, Stenosis 1 and Stenosis 2. In the present study, we only considered the impact of changes in the geometric size of the main stenosis in trachea. We defined this patient-specific model as the original model, Model 2, and exported it in the most common geometric output format, stereo-lithography interface format (STL) for virtual design of different stages of stenosis development.

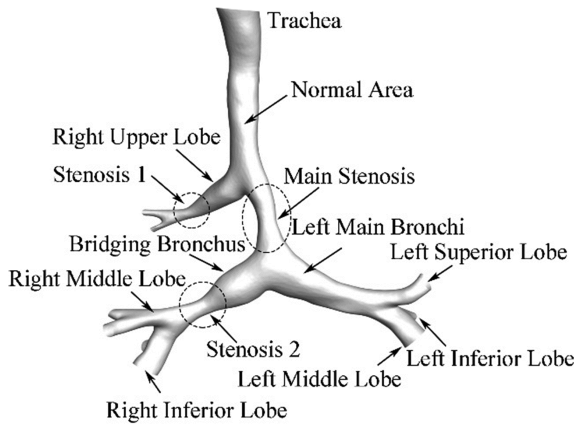


Fig. 1. Reconstruction of 3D patient-specific tracheal geometry

2.3 Model Rebuilding

The narrowest cross-sectional area of stenosis and the normal tracheal area can be determined by the imaging techniques. To calculate the stenosis ratio, we defined r as follows [8]:

$$r = \frac{S_N - S_S}{S_N} \times 100\% \quad (1)$$

S_N meant the normal tracheal area, and S_S expressed the narrowest cross-sectional area of main stenosis.

According to this definition, the stenosis ratio of patient's original model was about 60%. The original STL-formatted tracheal model was imported into computer-aided design (CAD) software Materialise[®]-3matic 10.0 and divided into three parts to geometrical design for the simulation of four stages of stenosis development as shown in Fig. 2. Then we modified the main stenosis to 0%, 20%, 40%, 80%, respectively to simulate four stages of stenosis development. Last, we integrated each part into a new model respectively. The Fig. 2 shows total five models in the present study: an original model (Model 2) with the stenosis ratio of 60%, Model 1 with the stenosis ratio of 80%, Model 3 with the stenosis ratio of 40%, Model 4 with the stenosis ratio of 20% and Model 5 with non-stenosis.

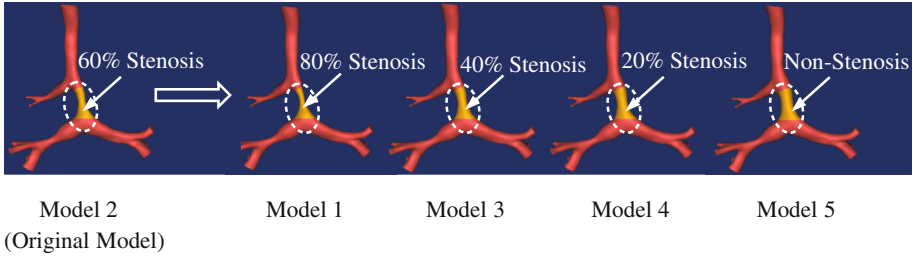


Fig. 2. Computer-aided design for model reconstruction

2.4 CFD Analysis

Governing equations of airflow. The airflow in trachea was assumed to be Newtonian and incompressible flow. Simulations were performed by solving the governing equations of the airflow including Navier-Stokes (N-S) and continuity equations [9], which were described as follows:

$$\frac{\partial}{\partial t}(\rho u_i) + \frac{\partial}{\partial x_j}(\rho u_i u_j) = -\frac{\partial p}{\partial x_i} + \frac{\partial}{\partial x_j} \left[u \left(\frac{\partial u_i}{\partial x_j} + \frac{\partial u_j}{\partial x_i} \right) \right] \quad (2)$$

$$\frac{\partial \rho}{\partial t} + \frac{\partial}{\partial x_j}(\rho u_j) = 0 \quad (3)$$

where ρ was the air density, μ was the viscosity, t was the time, u_i and u_j were the velocity vector of a point, p was the pressure, $i, j = 1, 2, 3$, x_i and x_j meant coordinate axes. We assumed the airflow with the constant density and viscosity in the present study ($\rho = 1.161 \text{ kg/m}^3$ [4], $\mu = 1.864 \times 10^{-5} \text{ kg/m s}$ [10]).

The Reynolds number, a dimensionless number, was used to characterize fluid flow, as defined in Eq. (4) [11]:

$$Re = \frac{\rho v d}{\mu} \quad (4)$$

where ρ and μ were air density and viscosity, v represented the velocity of airflow, and d was the characteristic length such as the diameter of the airway. We calculated the maximum Reynolds number was approaching to 3500. It suggested that the airflow in trachea should be the turbulence flow. In the present study, Wilcox $k-\omega$ model [12] was considered to obtain the turbulence viscosity for modeling the Reynolds stress, which was verified perfectly for airway flow simulations by CFD [13].

Mesh generation. In this step, we applied the grid-generation software, ANSYS®-ICEM 14.5, where five smoothed models with different stenosis ratio were imported. There were two types of grids in the fluid domain: three-layer body-fitted hexahedral grids and tetrahedral grids covering the remainder of the domain. Hereinto, an average nodal space of hexahedral grids increased by a ratio of 1.2. Grid independence

verification was performed in order to find the optimal number of grids for the efficient calculation. Table 1 lists the number of total elements and total nodes for each model.

Table 1. Mesh information for each model

	Total elements	Total nodes
Model 1 (80% Stenosis)	1,207,424	453,344
Model 2 (60% Stenosis)	1,229,095	459,218
Model 3 (40% Stenosis)	1,093,932	394,447
Model 4 (20% Stenosis)	1,232,199	460,201
Model 5 (Non-stenosis)	1,242,588	463,383

Boundary conditions and calculations. To imitate more practical airflow in the physiological conditions of trachea, we considered that the inlet boundary was extended 20 times of its diameter to develop velocity profile. Due to the serious CTS, ventilator (Maquent, Servo-I, Sweden) was applied in this patient. Figure 3 showed the data of the mass-flow from ventilator after the amendment in one respiration cycle. In addition, the outlet boundaries for the tracheal domain were extended 40 times of each diameter to obtain sufficient pressure recoveries, and a constant pressure of 0 atm was set at each outlet [14]. The tracheal walls, including the extended boundary walls, were assumed to be rigid with no-slip conditions.

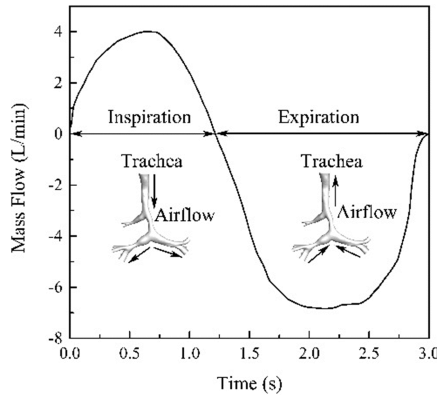


Fig. 3. Airflow mass flow rate in one respiration cycle

All of the above boundary conditions were set in the finite volume solver package, ANSYS®-FLUENT 14.5, which was utilized in simulate transient airflow of each tracheal model. The second-order upwind scheme and the semi-implicit (SIMPLE) method were chosen to solve the N-S equations. The convergence criteria were set to 10^{-5} for each time step.

3 Results

The stenosis ratios of Model 1, Model 2, Model 3, Model 4 and Model 5 were 80%, 60%, 40%, 20% and 0%. Among these models, Model 2 with 60% stenosis was original patient-specific trachea model and Model 5 with non-stenosis was normal trachea model without CTS used as control group. In this study, average pressure drop (APD) of the main stenosis, wall shear stress (WSS) and streamlines of airflow in each tracheal model, were calculated to evaluate the outcomes of five models varying different degrees of stenosis.

3.1 Average Pressure Drop

Airway resistance and ventilation efficiency can be objectively measured by APD. Therefore, APD of each main stenosis at the phase of inspiration and expiration were respectively calculated in Fig. 4. Through comparisons of these values of each model's APD, it was obvious that APD decreased nonlinearly whether at the phase of inspiration or expiration with the decreasing degree of stenosis. And assuming under the same respiratory cycle, it is normal that the value of APD at the phase of inspiration was lower than that at the phase of expiration in each model. This indicated that its workload of expiration was heavier, and it's easier to lead to airway closure and airflow obstruction at this phase. Particularly there was a sharp decrease obtained between Model 1 and Model 2. And the change of the values of APD between two adjacent models was relatively steady in Model 3, Model 4 and Model 5.

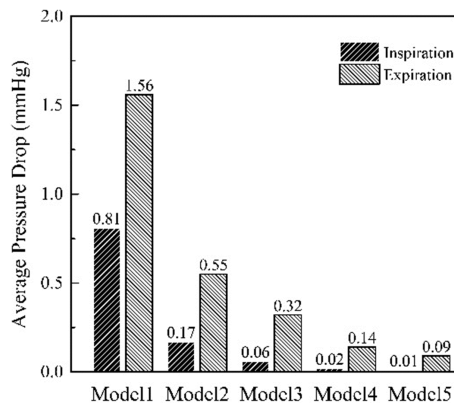


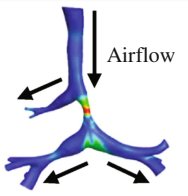
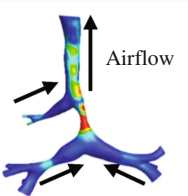
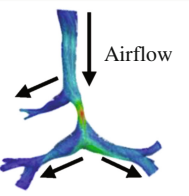
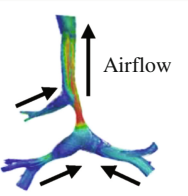
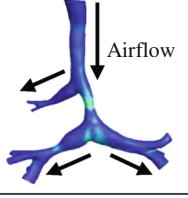
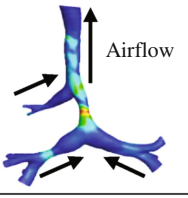
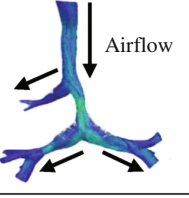
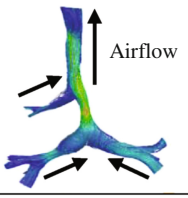
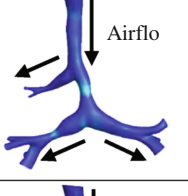
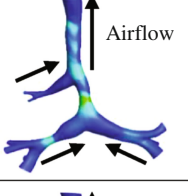
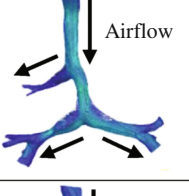
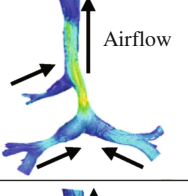
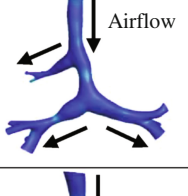
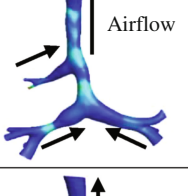
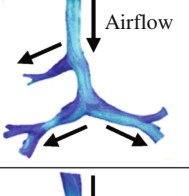
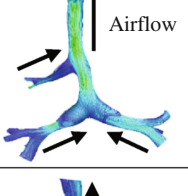
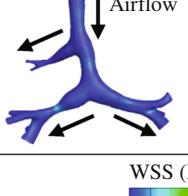
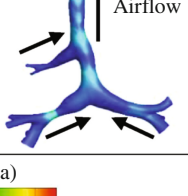
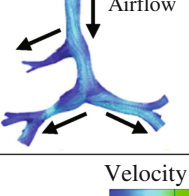
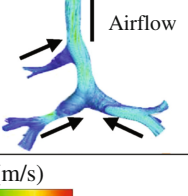


Fig. 4. Average pressure drop at main stenosis at the phase of inspiration and expiration

3.2 Wall Shear Stress

WSS of tracheal wall was regarded as a measurement of the interaction between the air flow and the boundary of the airway. Many studies have demonstrated that much high WSS would damage to the tracheal wall and further cause many diseases. In Table 2,

the closer the color of the tracheal wall was to the blue, the smaller the value of WSS was. If it is closer to the red, the value of WSS increased. As we can see, all the highest WSS of each model occurred in main stenosis. With the decrease of stenosis ratio, change of WSS between Model 1 and Model 2 is particularly evident, and there was no significant difference between other models. In comparison with expiration phase, WSS in inspiration phase was much lower.

Table 2. Wall shear stress (WSS) and aerodynamic analysis (streamlines)

	WSS		Streamline	
	Inspiration	Expiration	Inspiration	Expiration
Model 1				
Model 2				
Model 3				
Model 4				
Model 5				
Legend	WSS (Pa)  0 1 2 3 4 5 6		Velocity (m/s)  0 4 8 12 16 20	

3.3 Streamlines

Table 2 displayed the streamlines at the maximum velocity of airflow at the inspiration phase and expiration phase as well. The higher value of velocity was observed in the main stenosis of the model 1. With the stenosis decreased, the velocity of airflow in the main stenosis slowed down. Accompanied by an increase of stenosis at the phase of inspiration, the size of turbulence became larger and the velocity of airflow was very small, which indicated resistance in the area of BB was getting stronger. And large rotating flow of each model was created area of BB to trachea at the phase of expiration. The velocity varied from Model 1 to Model 2 significantly, which was evidenced from another side to indicate it is critical timing for surgical correction.

4 Discussion

CTS is one of congenital tracheal diseases characterized by uncommon, complex, and potentially life-threatening, which could lead to pulmonary infection and respiration insufficiency. In the wake of the development in science and technology, the survival of CTS has greatly improved. One reason may be that the methods of diagnosis are becoming more diverse and accurate, such as bronchoscopy, bronchography and multi-detector computed tomography (MDCT) [15, 16], which could only provide the static imagine modalities of the main airway and is unavailable to the dynamic information. Surgeons usually depend on the results of above methods of diagnosis and their own previous experience to choose the surgical timing for the children with CTS. However, the optimal and exact timing for surgical intervention is still controversial. If it can be predicted, the operative survival rate of CTS would be definitely greatly improved.

In the present study, we utilized medical imagining software to generate 3D patient tracheal model with CTS from high resolution CT 2D images to 3D models, and CAD to rebuild four models with different stenosis based on the original 3D stenosis model. The aerodynamics of five models was calculated by using CFD. Several parameters including APD, WSS and streamlines were calculated to estimate aerodynamics of five models. Airway resistance and efficiency of ventilation can be measured objectively by APD. In the outcomes of APD, the general trend was that the values of APD declined as the degree of stenosis decreased, showing a nonlinear reducing. It was a direct proof of the degree of stenosis on the APD great impact and reasonable that airway resistance became lower as well as ventilation efficiency was getting higher with decrease of the stenosis ratio. The stenosis ratio was positively correlated with APD and the value of APD when in an inspiration phase was lower than that when in an expiration phase in each model, which were consistent with clinical practice. Moreover, there was a sharp decrease obtained between Model 1 and Model 2. Abnormal increase of APD disclosed that normal work of respiratory muscle can't meet the physiological needs. It would lead the patient to have symptoms like breathing difficulties, wheezing or even suffocation. It suggested surgical correction was necessary for the investigated patient with 60% tracheal stenosis.

WSS was regarded as a measurement of an interaction between the moving fluid and the solid wall, which was displayed in Table 2. High value of WSS appeared in main

stenosis parts, which would cause additional destruction of the bronchial epithelium. Through the longitudinal observation from top to bottom, WSS in main stenosis gradually decreased both in the inspiratory phase and expiration phase. As stenosis ratio declined, airflow resistance became lower, which led to decreases WSS and strengthened interaction between the airflow and the wall of trachea in two phases, respectively. It was observed that WSS of main stenosis in the inspiratory phase were lower respectively than that at the expiration phase due to higher workload in the expiration phase. Similarly, change of WSS between Model 1 and Model 2 is particularly evident. The velocity varied from 80% stenosis to 60% stenosis significantly along with the decrease of stenosis ratio, which was evidenced that 60% stenosis is an inflection point for this patient from another side. Therefore, we should attach importance to this critical inflection point that can predict the critical timing of surgery.

5 Conclusion

Development of tracheal stenosis have great effects on the outcomes of aerodynamics. The combination with the technique of CFD and CAD is a potential tool for surgical timing prediction to minimize the surgical risk. APD, WSS, and streamlines are critical parameters for evaluation aerodynamics characteristics of airflow in trachea.

Acknowledgement. We have been genuinely appreciative of the support of the National Nature Science Foundation of China (No. 81602818, P.I.: Limin Zhu and No. 81501558, P.I.: Jinlong Liu), the Project-sponsored by the Scientific Research Foundation for the Returned Overseas Chinese Scholars, State Education Ministry (No. 20144902, P.I.: Jinlong Liu), the Fund of The Shanghai Committee of Science and Technology (No. 15411967100, P.I.: Limin Zhu and No. 14411968900, P.I.: Jinlong Liu) and the Biomedical and Engineering (Science) Inter-disciplinary Study Fund of Shanghai Jiaotong University (No. YG2014MS63, P.I.: Jinlong Liu).

References

1. Chung, S.R., Yang, J.H., Jun, T.G., et al.: Clinical outcomes of slide tracheoplasty in congenital tracheal stenosis. *Eur. J. Cardio-Thorac. Surg.* **47**(3), 537–542 (2015)
2. Grillo, H.C., Wright, C.D., Vlahakes, G.J., et al.: Management of congenital tracheal stenosis by means of slide tracheoplasty or resection and reconstruction, with long-term follow-up of growth after slide tracheoplasty. *J. Thorac. Cardiovasc. Surg.* **123**(1), 145–152 (2002)
3. Hofferberth, S.C., Watters, K., Rahbar, R., et al.: Management of congenital tracheal Stenosis. *Pediatr.* **136**(3), e660–e669 (2015)
4. Mimouni-Benabu, O., Meister, L., Giordano, J., Fayoux, P., Loundon, N., et al.: A preliminary study of computer assisted evaluation of congenital tracheal stenoses: a new tool for surgical decision-making. *Int. J. Pediatr. Otorhinolaryngol.* **76**, 1552–1557 (2012)
5. Chen, F.L., Horng, T.L., Shih, T.C.: Simulation analysis of airflow alteration in the trachea following the vascular ring surgery based on CT images using the computational fluid dynamics method. *J. Xray Sci. Technol.* **22**, 213–225 (2014)
6. Cebra, J.R., Summers, R.M.: Tracheal and central bronchial aerodynamics using virtual bronchoscopy and computational fluid dynamics. *IEEE Trans. Med. Imaging* **23**(8), 1021–1033 (2004)

7. Gemci, T., Ponyavin, V., Chen, Y., et al.: Computational model of airflow in upper 17 generations of human respiratory tract. *J. Biomech.* **41**(9), 2047–2054 (2008)
8. Liu, J.L., Itatani, K., Shiurba, R., et al.: Image-based computational hemodynamics of distal aortic arch recoarctation following the Norwood procedure. In: *International Conference on Biomedical Engineering and Informatics*. IEEE, 318–323. (2011)
9. Detta, R.A.K., Ducharme, N.G., Pease, A.P.: Simulation of turbulent airflow using a CT based upper airway model of a racehorse. *J. Biomech. Eng.* **130**(3), 13 (2008)
10. Chien-Yi, H., Liao, H.M., Tu, C.Y., et al.: Numerical analysis of airflow alteration in central
11. Chang, H.K., Mortola, J.P.: Fluid dynamic factors in tracheal pressure measurement. *J. Appl. Physiol. Respir. Environ. Exerc. Physiol.* **51**(1), 218–225 (1981)
12. Wilcox, D.C.: Reassessment of the scale determining equation for advanced turbulence models. *J. Am. Inst. Aeronaut. Astronaut.* **26**(11), 1299–1310 (1988)
13. Mylavarapu, G., Murugappan, S., Mihaescu, M., Kalra, M., Khosla, S., Gutmark, E.: Validation of computational fluid dynamics methodology used for human upper airway flow simulations. *J. Biomech.* **42**, 1553–1559 (2009)
14. Zhu, L., Liu, J., Zhang, W., et al.: Computational aerodynamics of long segment congenital tracheal stenosis with bridging bronchus. In: *Asian Control Conference*, pp. 1–5. (2015)
15. Baden, W., Schaefer, J., Kumpf, M., Tzaribachev, N., Pantalitschka, T., Koitschev, A., Ziemer, G., Fuchs, J., Hofbeck, M.: Comparison of imaging techniques in the diagnosis of bridging bronchus. *Eur. Respir. J.* **31**(5), 1125–1131 (2008)
16. Zhong, Y.M., Jaffe, R.B., Zhu, M., Gao, W., Sun, A.M., Wang, Q.: CT assessment of tracheobronchial anomaly in left pulmonary artery sling. *Pediatr. Radiol.* **40**(11), 1755–1762 (2010)